Geometry of phase and polarization singularities, illustrated by edge diffraction and the tides

Michael Berry

H.H. Wills Physics Laboratory, Tyndall Avenue, Bristol BS8 1TL, United Kingdom

ABSTRACT

In complex scalar fields, singularities of the phase (optical vortices, wavefront dislocations) are lines in space, or points in the plane, where the wave amplitude vanishes. Phase singularities are illustrated by zeros in edge diffraction and amphidromies in the heights of the tides. In complex vector waves, there are two sorts of polarization singularity. The polarization is purely circular on lines in space or points in the plane (C singularities); these singularities have index ±1/2. The polarization is purely linear on lines in space for general vector fields, and surfaces in space or lines in the plane for transverse fields (L singularities); these singularities have index ±1. Polarization singularities (C points and L lines) are illustrated in the pattern of tidal currents.

Keywords: amphidromies, edge diffraction, fields, phase, polarization, Sommerfeld solution, singularities, waves.

1. INTRODUCTION

Recently, experimental and theoretical interest in phase singularities has revived and intensified [1, 2]. This is part of what has come to be called (following Soskin) *singular optics*. Interpreted properly in its full generality, singular optics is the study of the geometrical singularities that arise at each level of description in the physics of light (or - still more generally, in any branch of the physics of waves). At the geometrical level, the singularities are caustics, that is, envelopes of families of rays. At the level of scalar optics, the singularities are wavefront dislocations of the phase (otherwise called optical vortices or topological charges). And in vector waves the singularities are in the patterns of polarization. A general review, with many references, has been published by Nye [3]. Here I will concentrate on the phase and polarization singularities, with a twofold aim.

The first purpose is to review these singularities and some associated concepts, and provide a convenient collection of (mostly) known formulas. Section 2 deals with scalar waves (where in the general theory we follow the notation in [4]) and section 5 deals with vector waves (where in the general theory we follow the notation in [25]).

The second purpose is to provide some historical perspective by illustrating how far back in the history of science these ideas can be traced. Section 3 deals with edge diffraction [5]; the story spans more than three centuries, starting with Grimaldi and Newton and culminating in the currently-popular Madelung ('Bohmian') formalism for waves. Edge diffraction also illustrates some important features of phase singularities. Sections 4 and 6 deal with the tides, which are not only important physical phenomena in their own right [6] but also provide transparent illustrations of the physics of complex scalar and vector fields, and the associated singularities.

For simplicity I will concentrate only on monochromatic waves, so there will be a (usually) implicit time factor $\exp(-i\omega t)$. However, the ideas apply equally to waves that are changing with time, for example signals - indeed phase singularities were discovered in this way [7].

2. PHASE SINGULARITIES IN SCALAR FIELDS

As a function of position $\mathbf{r}$ in two or three dimensions (that is, $\mathbf{r}=\{x,y,z\}$ or $\mathbf{r}=\{x,y\}$, we consider complex scalar waves

$$\psi(\mathbf{r}) = \rho(\mathbf{r}) \exp\{\mathrm{i}\chi(\mathbf{r})\} = \xi(\mathbf{r}) + \mathrm{i}\eta(\mathbf{r}), \tag{1}$$

with modulus ρ and phase χ, and real and imaginary parts ξ and η (we will usually omit the **r** dependence). Our interest here is in the wavefronts, defined as the surfaces (or in two dimensions the curves) where the phase $\chi(\mathbf{r})$=constant (mod 2π), and in particular the singularities of the wavefronts. In free space, or in a medium without singularities, $\xi(\mathbf{r})$ and $\eta(\mathbf{r})$, and hence $\psi(\mathbf{r})$, are smooth functions of position. Therefore the phase can be singular only if the modulus ρ vanishes, and since ρ=0 implies two conditions (ξ=0 and η=0), the phase singularities are lines in space (threads of darkness), and points in the plane.

During a circuit of a phase singularity, the phase changes by a multiple of 2π; generically, that is almost always, the multiple is ±1. This change can be understood in terms of the current vector

$$\mathbf{j} = \mathrm{Im}\,\psi^* \nabla\psi = \rho^2 \nabla\chi = \xi\nabla\eta - \eta\nabla\xi. \tag{2}$$

Close to a singularity, lines of **j** are circles centred on the singularity [4], giving rise to the term *optical vortices* to describe the singular lines. The direction **n** of a vortex line is that of the associated vorticity, that is

$$\mathbf{\Omega} = \mathbf{n}|\mathbf{\Omega}| = \tfrac{1}{2}\nabla\wedge\mathbf{j} = \tfrac{1}{2}\,\mathrm{Im}\,\nabla\psi^*\wedge\nabla\psi = \nabla\xi\wedge\nabla\eta. \tag{3}$$

In three dimensions, $\mathbf{\Omega}$ defines a natural sense for the singularity, with respect to which the phase increases (that is, the phase change is $+2\pi$). In the plane, it is more natural to define the phase change relative to the fixed normal to the plane, leading to the notion of the strength (*topological charge*) of the singularity, whose value ±1 is given by

$$S = \mathrm{sgn}\left(\partial_x\xi\partial_y\eta - \partial_y\xi\partial_x\eta\right) \tag{4}$$

(for further discussion of this point, see [8, 9]).

Although the **j** lines are circles surrounding the singularity, the phase usually varies nonuniformly. This variation - the local structure of the singularity - is naturally described [4] by the same ellipse that gives the local form of the ρ contours, determined by the quadratic form

$$\rho^2 = (\nabla\xi\cdot\mathbf{R})^2 + (\nabla\eta\cdot\mathbf{R})^2, \tag{5}$$

where **R** describes position in a plane transverse to the singularity, with **R**=0 at the singularity. The phase lines are concentrated near the major axis of this ellipse, and sparse near the minor axis.

In three dimensions, the phase may change along the singular line as well as around it. Then the wavefront surfaces close to the singularity are helicoids, analogous to surfaces defined by atomic planes in a crystal, and this is why lines of phase singularity are also called *wavefront dislocations*. A singularity where χ does not vary along the line is an edge dislocation. If χ does vary along the line, the singularity has screw character. For waves in free space, a local measure of screwness (developing an idea in [10]) is the rate at which χ varies along the direction **n** of the dislocation (we call this the *z* direction), measured in units of the free-space wavenumber *k*. Since this variation can depend on the azimuth ϕ round the line, it is convenient to average over ϕ. Thus a possible definition of the screwness σ is

$$\sigma = \frac{1}{k}\langle\chi'\rangle_{\phi\,\mathrm{average}} \equiv \lim_{\mathbf{R}\to 0} \frac{\int_0^{2\pi} \mathrm{d}\phi\,\rho^2(\mathbf{R})\chi'(\mathbf{R})}{k\int_0^{2\pi}\mathrm{d}\phi\,\rho^2(\mathbf{R})} = \lim_{\mathbf{R}\to 0}\frac{\int_0^{2\pi}\mathrm{d}\phi\, j_z(\mathbf{R})}{k\int_0^{2\pi}\mathrm{d}\phi\,\rho^2(\mathbf{R})} = \lim_{\mathbf{R}\to 0}\frac{\int_0^{2\pi}\mathrm{d}\phi\left(\xi(\mathbf{R})\eta'(\mathbf{R}) - \eta(\mathbf{R})\xi'(\mathbf{R})\right)}{k\int_0^{2\pi}\mathrm{d}\phi\left(\xi^2(\mathbf{R})+\eta^2(\mathbf{R})\right)}, \tag{6}$$

where the primes denote *z* derivatives. The limit is delicate because **R** must be taken close to the dislocation line but the derivatives must be taken along the direction of the line itself; otherwise, the component j_z will vanish because **j** is perpendicular to the local vorticity $\mathbf{\Omega}$ (cf. (2) and (3)). Exploiting the fact that ψ varies linearly away from its zero on the dislocation line, we can evaluate the average and take the limit explicitly, and obtain, after a short calculation, the nonsingular expressions

$$\sigma = \frac{\nabla\xi\cdot\nabla\eta' - \nabla\eta\cdot\nabla\xi'}{k\left((\nabla\xi)^2 + (\nabla\eta)^2\right)} = \frac{\mathrm{Im}\nabla\psi^*\cdot\nabla\psi'}{k|\nabla\psi|^2}. \tag{7}$$

For an edge dislocation, σ=0, while for a pure screw dislocation, σ=±1. It is important to appreciate that the concept of screwness is essentially three-dimensional, and has no meaning for dislocation points in the plane. Thus, the continuously variable quantity σ, describing how χ varies along the dislocation, is unrelated to the (integer) dislocation strength *S*, which describes how χ varies around the disclocation.

3. NEWTON AND EDGE DIFFRACTION: A NEAR MISS AND AN ASTONISHING ANTICIPATION

In 1717, Isaac Newton [11] speculated on a matter that had disturbed him for half a century, namely the discordance between his corpuscular theory of light and observations that we now interpret as clear evidence for the wave nature of light, in particular Grimaldi's experiments in the 1660s on diffraction by an edge. Newton conjectured that the edge exerts an attractive force on the light, bending its rays into the geometrical shadow. To explain the observation of several fringes near the geometrical shadow, he asked:

Query 3: Are not the rays of Light in passing by the edges and sides of Bodies, bent several times backward and forwards, with a motion like that of an Eel? And do not the three Fringes of colour'd Light above-mentioned arise from three such bendings?

From a modern perspective, Newton's explanation is exactly correct, if his rays are interpreted as the streamlines of ψ, that is, the lines of current $\mathbf{j}$. It has taken a long time to reach this understanding. First, two centuries elapsed before Sommerfeld's exact solution, in 1896 [5], of the diffraction of waves by a half-plane. For incident waves travelling in the positive *x* direction from x=-∞, with the diffracting half-plane defined by x=0, y <0 (i.e. the edge is at x=y=0), Sommerfeld's solution is, in units of 2π/wavelength (i.e. k=1)

$$\begin{gathered}\psi(\mathbf{r}) = \exp\left(-\tfrac{1}{4}\,\mathrm{i}\pi\right)\left[\exp(\mathrm{i}x)F\{u_-(\mathbf{r})\} + \alpha\exp(-\mathrm{i}x)F\{u_+(\mathbf{r})\}\right] \\ \alpha = +1\left(\text{Neumann boundary conditions}\right);\ \alpha = -1\left(\text{Dirichlet boundary conditions}\right);\ \alpha = 0\ \left(\text{black screen}\right),\end{gathered} \tag{8}$$

where *F* denotes the Fresnel integral

$$F(u) = \int_u^\infty \mathrm{d}t\,\exp\left\{\mathrm{i}\pi t^2\right\}, \tag{9}$$

and, in polar coordinates r,ϕ, defined so the edge is at ϕ=-π/2 and +3π/2,

$$u_-(\mathbf{r}) = -\sqrt{\frac{2r}{\pi}}\sin\tfrac{1}{2}\phi, \quad u_+(\mathbf{r}) = \sqrt{\frac{2r}{\pi}}\cos\tfrac{1}{2}\phi. \tag{10}$$

The first and second terms in (8) represent the incident and reflected waves respectively, together with associated diffracted edge waves (though we note that other interpretations are possible [12]).

A further half-century elasped before detailed computations [13] revealed the rich structure of Sommerfeld's solution, in the Neumann case. Figure 1a shows the wave intensity in the Dirichlet case, clearly indicating the fringes that so intrigued Newton. Figure 1b shows the streamlines, displaying the eel-like undulations precisely as Newton predicted. (These streamlines are conveniently computed as contours of the stream function - whose existence is guaranteed by $\nabla\cdot\mathbf{j} = 0$ - namely $s(r,\phi) = -\int_0^r \mathrm{d}r'\mathrm{Im}\,\psi^*(r',\phi)\partial_\phi\psi(r',\phi)/r'$.)

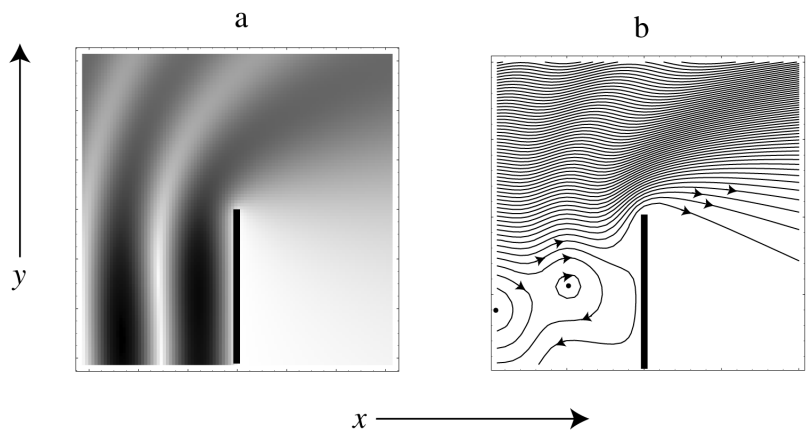

Figure 1**.** Sommerfeld edge-diffracted wave (8), for Dirichlet boundary conditions. (a) Density plot of wave intensity, proportional to darkness of shading, so the dislocation is visible as a bright spot in front of the screen; (b) streamlines, showing newton's 'eel' undulations and the loop surrounding the dislocation point.

What of the 'force' postulated by Newton to account for the deflection and undulations of the rays? This was discovered only in 1926, in the context of the 'hydrodynamic' formalism for quantum mechanics [14] - though the explanation applies to waves of all sorts. If wave equations are reformulated in terms of $\mathbf{j}$ and ρ, rather than ψ, the streamlines are influenced nonlocally by a 'quantum potential' in addition to any local forces incorporated in the hamiltonian. (Recently, the Madelung formalism has become popular as an interpretation of quantum theory, under the name 'Bohmian mechanics'[15].)

So, Newton was right in every respect. However, he appears not to have imagined that the forces could be strong enough to bend the rays into closed orbits. If he had taken this taken this further step, he would be celebrated as the discoverer of optical vortices. Closed streamlines do not occur in diffraction from a black (nonreflecting) screen, because the interference

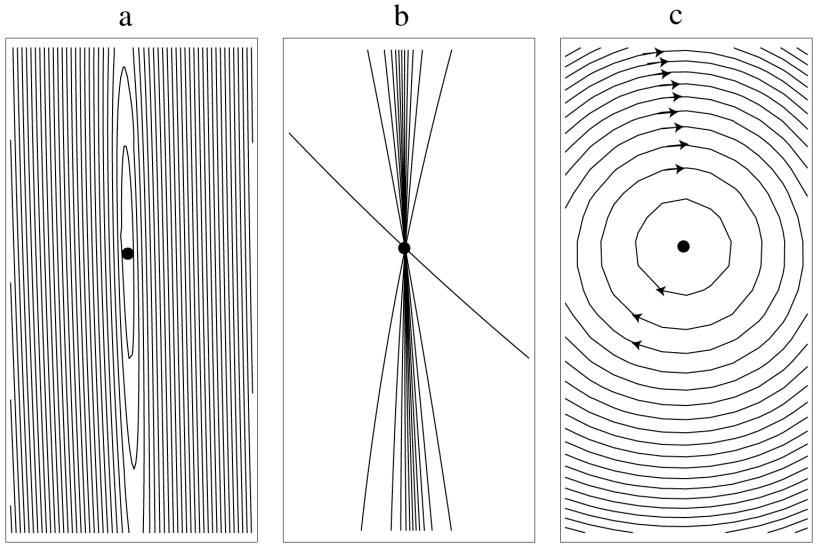

Figure 2. Magnification of dislocation in figure 1. (a) Contour plot of wave intensity, showing highly anisotropic elliptic structure near the zero; (b) wavefronts at intervals of 15˚, showing concentration along the ellipse axis; (c) streamlines, showing circular structure near the dislocation.

between the incident and edge-diffracted waves is too weak to generate zeros. However, with reflecting screens (Dirichlet or Neumann), the additional reflected wave produces points of complete destructive interference. One of these is visible on figure 1b. From the magnifications in figure 2, it is clear that although the streamlines are circles the local intensity and phase structures are highly anisotropic. In the present case, this anisotopy has its origin in the fact that in the absence of the edge (that is, for an infinite screen rather than a half-plane), destructive interference between incident and reflected waves would occur on degenerate dark fringes in the form of lines (in two dimensions); the perturbation from the edge-diffracted waves breaks the degeneracy, leaving long narrow low-intensity valleys, reaching zero only at isolated points.

4. WHEWELL AND THE TIDES: THE FIRST PHASE SINGULARITY

In the world's oceans, the tides are waves driven by the gravitation of the moon and the sun. This gives rise to complicated astronomical periodicities, with many fourier components. The fundamental explanation of the tides was given by Newton, and the dynamical equations governing the water, in particular the displacement of its surface, were given by Laplace [6]. By the early nineteenth century, good explanations had been constructed for the tides on an ideal ocean of constant depth, covering an imaginary spherical earth with no land, and for the different periodicities. Here we need consider only the dominant contribution, called the M_2 tide, which is the semidiurnal tide from the moon, with a period of 12.42h.

On the real oceans, the heights of the tides vary in complicated ways from place to place, and in the 1830s this was the subject of extensive studies [16, 17] by William Whewell. The aim was

"...to connect the actual tides of all the different parts of the world - and to account for their varieties and seeming anomalies..."

Whewell realised that much of the complication is due to interference between waves reaching the same part of the ocean by different routes, and perceived that an intelligible picture of the tides would be provided by what we would nowadays call the wavefronts of the tide wave. He called these cotidal lines, and defined them as follows:

"...we may draw a line through all the adjacent parts of the ocean which have high water at the same time; for instance, at 1 o'clock on a given day. We might draw another line through all the places which have high water at 2 o'clock on the same day. Such lines may be called *cotidal lines*; and these will be the principal subject of the present essay."

A particular problem arose in connecting the observations of tides on the British and continental sides of the North Sea (then called the German Ocean) in order to discover the form of the wavefronts over this sea. Here is Whewell's brilliant solution:

"It appears that we may best combine all the facts into a consistent scheme, by dividing this ocean into two *rotatory* systems of tide-waves...[in each space] the cotidal lines may be supposed to rotate round [a point] where there is no tide, for it is clear that at a point where all the cotidal lines meet, it is high water equally at all hours, that is, the tide vanishes."

In other words, the North Sea contains two points of phase singularity! Whewell's map is reproduced in figure 3. These oceanic dislocations were later called *amphidromies*. Their identification and calculation (using Laplace's dynamical equations together with observations of tides round the coasts of the world's oceans) are central in modern studies of the tides [6]. In oceanographic models, the positions of amphidromies are extraordinarily sensitive to changes in the depth of the oceans [18], reflecting the fact (well known in optical applications [19]) that phase singularities are the most delicate features of waves, even though they are generic, that is, structurally stable in the mathematical sense. All the main bodies of water on the earth possess amphidromies; figure 4 shows a perfect specimen close to Crimea, where the singular optics conferences of 1997 and 2000 were held.

The mathematical interpretation of Whewell's argument gives a fine illustration of the formalism developed in section 2, with the water surface $z(\mathbf{r},t)$ written in terms of the complex wave $\psi(\mathbf{r})$ as

$$z(\mathbf{r},t) = \mathrm{Re}\left[\psi(\mathbf{r},t)\exp(-\mathrm{i}\omega t)\right] = \rho(\mathbf{r})\cos\left(\chi(\mathbf{r}) - \omega t\right). \tag{11}$$

Why must ψ be complex? Because the high tide must move across the ocean, according to the law $\chi(\mathbf{r})$-ωt=0 (mod 2π). If $\psi(\mathbf{r})$ were a real function, the time-dependence would be just $\cos(\omega t)$, and the phase of the tidal oscillations in the height of the

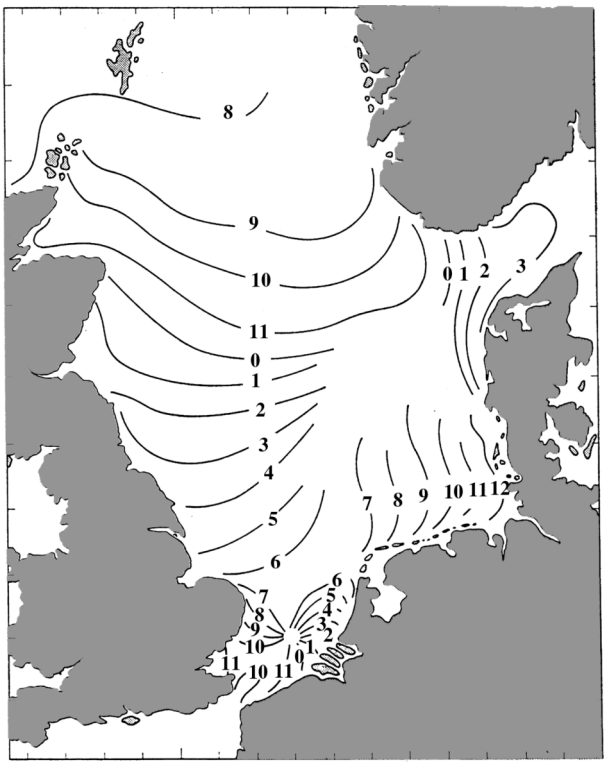

Figure 3. Whewell's map of the cotidal lines in the North Sea, showing two amphidromies (after [17]).

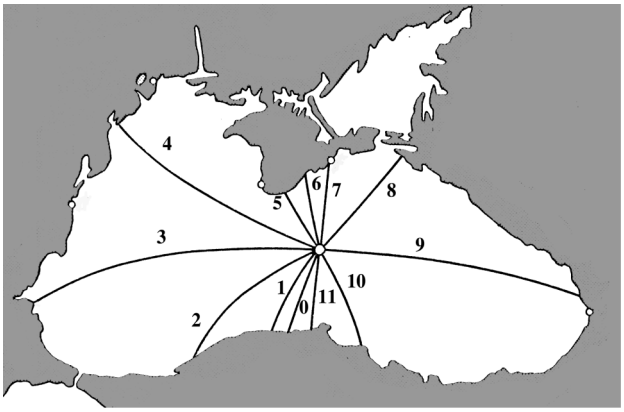

Figure 4. Amphidromy in the Black Sea (after [18]).

water would be the same everywhere: the tide wave would not travel. Precisely such correlated oscillations occur in, for example, the vibrations of a membrane, where the spatial variation of a mode is described by a real function $\psi(\mathbf{r})$; for such a mode in two dimensions, the zeros are nodal lines rather than dislocation points. Both type of wave motion are *steady*, in the sense that the time-dependence is harmonic. In addition, the modal vibration of a membrane is a *standing* wave: its time-dependence is the same everywhere. By contrast, the tide wave is steady but not standing.

Still the fundamental question can be asked: what is the physical reason why the tide waves are merely steady, while the vibrations of a membrane are not just steady but also standing. The answer is an extension of an argument more familiar in quantum mechanics, and involves time-reversal symmetry (T). Complex waves are inevitable whenever T is broken. In

membranes, the physics possesses T, and the modes are real. In the tides, however, the rotation of the earth breaks T (the earth rotates from west to east, not vice versa), and so the waves are complex. (A quantum example of stationary states where the modes are represented by complex functions $\psi(\mathbf{r})$ occurs in the presence of magnetic fields, and explicit calculations [20, 21] for such waves in the plane show the expected presence of dislocation points rather than nodal lines.)

Whewell's notion of amphidromes in the pattern of cotidal lines was not immediately accepted. Airy [22] regarded the tideless point singularities as mathematically impossible, and proposed an incoherent alternative (figure 5), involving crossing cotidal lines, that was reproduced uncritically for many decades. The source of Airy's scepticism is not clear, especially in view of his high level of mathematical sophistication. It has been suggested [6] that his misunderstanding was based on a confusion between tide heights and tidal currents (see section 6); another possibility is that Airy had in mind interference as it occurs in membrane vibrations, involving real waves and therefore nodal lines rather than dislocation points. In any case, Whewell's map of the cotidal lines in the North Sea, complete with amphidromies, has been completely vindicated by modern calculations [23] and direct measurements of $z(\mathbf{r},t)$ from satellites.

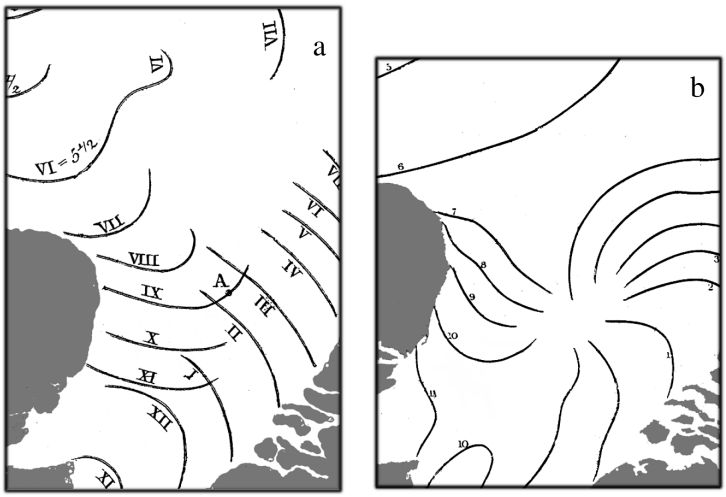

Figure 5. Airy's erroneous alternative [22](a) to Whewell's map of cotidal lines (b) (magnification of figure 3).

5. POLARIZATION SINGULARITIES IN VECTOR FIELDS

Consider now the complex vector field

$$\mathbf{E}(\mathbf{r}) = \mathbf{P}(\mathbf{r}) + \mathrm{i}\mathbf{Q}(\mathbf{r}) \tag{12}$$

constructed from the two real fields **P** and **Q**. **E** could represent the electric or magnetic field of light, or, as we shall see in the next section, the current of the tide. From **E** can be generated the real time-harmonic field

$$\mathrm{Re}\left(\mathbf{E}\exp\left(-\mathrm{i}\omega t\right)\right) = \mathbf{P}\cos\omega t + \mathbf{Q}\sin\omega t. \tag{13}$$

At each point **r** in two or three dimensions, this vector describes an ellipse in the plane of **P**(**r**) and **Q**(**r**). This is the *polarization ellipse* of **E**. It is characterized by its normal vector

$$\mathbf{N}_\mathrm{e} \equiv \left|\mathbf{N}_\mathrm{e}\right|\mathbf{n}_\mathrm{e} = \tfrac{1}{2}\,\mathrm{Im}\,\mathbf{E}^* \wedge \mathbf{E} = \mathbf{P} \wedge \mathbf{Q} \tag{14}$$

and by the orthogonal directions of its semiaxes, for which a short calculation gives the formulas

$$\mathbf{E}_{+} = \frac{\mathrm{Re}\,\mathbf{E}^{*}\sqrt{\mathbf{E}\cdot\mathbf{E}}}{\left|\sqrt{\mathbf{E}\cdot\mathbf{E}}\right|} = \frac{\mathrm{Re}(\mathbf{P}-\mathrm{i}\mathbf{Q})\sqrt{P^2-Q^2+2\mathrm{i}\mathbf{P}\cdot\mathbf{Q}}}{\left(\left(P^2-Q^2\right)^2+4(\mathbf{P}\cdot\mathbf{Q})^2\right)^{1/4}},$$
$$\mathbf{E}_{-} = \frac{\mathrm{Im}\,\mathbf{E}^{*}\sqrt{\mathbf{E}\cdot\mathbf{E}}}{\left|\sqrt{\mathbf{E}\cdot\mathbf{E}}\right|} = \frac{\mathrm{Im}(\mathbf{P}-\mathrm{i}\mathbf{Q})\sqrt{P^2-Q^2+2\mathrm{i}\mathbf{P}\cdot\mathbf{Q}}}{\left(\left(P^2-Q^2\right)^2+4(\mathbf{P}\cdot\mathbf{Q})^2\right)^{1/4}}. \qquad (15)$$

(These expressions are invariant under change of the overall phase of **E**, as they must be in order to represent a fixed ellipse.) Alternatively stated, $\mathbf{E}_{\pm}$ are the two eigenvectors of the matrix $P_iP_j+Q_iQ_j$ that correspond to nonzero eigenvalues, where *i* and *j* denote the components of **P** and **Q** (in three dimensions there is a zero eigenvalue). The three orthogonal vectors $\mathbf{N}_e$, $\mathbf{E}_+$, $\mathbf{E}_-$ form a frame at each point **r**.

Since a complex vector field is represented by a field of ellipses, the vector counterpart of phase singularities are the polarization singularities that can occur in fields of ellipses. In the general three-dimensional case these have been classified by Nye [3, 24, 25]. There are two sorts of singularity.

The first occurs at places **r** where the ellipses degenerate to circles, that is, where the vectors **P** and **Q** have the same length and are perpendicular. These are called C singularities, characterized by

$$\mathbf{E}\cdot\mathbf{E} = P^2+Q^2+2\mathrm{i}\mathbf{P}\cdot\mathbf{Q} = 0 \quad (\text{C singularity}). \qquad (16)$$

For a circle, the axes are undefined, and indeed the formulas (15) become degenerate when $\mathbf{E}\cdot\mathbf{E}=0$. The condition (16) consists of two equations, so C singularities are *lines* in three dimensions and *points* in two dimensions. This is reminiscent of the phase singularities of scalar fields, and indeed the C singularities in **E** are the dislocations of the scalar field $\psi = \mathbf{E}\cdot\mathbf{E}$.

A C singularity is characterized by the pattern of (almost circular) polarization ellipses close to it. The possible patterns are more complicated than the wavefronts that radiate from a dislocation. There are three geometrically distinct generic (that is, stable under perturbation) patterns, called the star, lemon, and monstar [24, 26, 27]. To illustrate them, it is convenient to draw the orthogonal net of lines corresponding to the two direction fields $\mathbf{E}_{\pm}$ in the plane perpendicular to $\mathbf{N}_e$, and these are depicted in figure 6. Obviously the C singularity is a singularity in this net, because the ellipse axes are undefined there. In transverse (two-dimensional) vector waves, the lemon and star singularities (but not, curiously, the monstar) are familiar in the patterns of isogyres [28] (see also [29] for a simple example). Analogous to the index +1 of a dislocation is the index of a C singularity, defined as the number of rotations of the associated directions in a circuit of the singularity. For the lemon and monstar, the index is +1/2, and for the star the index is -1/2. (In scalar waves, the index -1 corresponds to phase saddles [30]). An additional characterization of C singularities, with no counterpart for dislocations, is the number of lines (in each of the two orthogonal families) passing through the singularity. For the lemon this is 1, and for the star and monstar it is 3. As an example, the following field displays all three C singularities at $\mathbf{r}=0$:

$$\mathbf{E} = \{1+\mathrm{i}by, \mathrm{i}(1-x)\} \qquad (17)$$

(the singularities are star for $b<0$, lemon for $0<b<2$, and monstar for $b>2$). The C analogue of the strength *S* of a dislocation is the sense of rotation of the vector (13) round its ellipse, that is, whether the circular polarization is right- or left-handed.

In three dimensions, a C line need not be parallel to the ellipse normal $\mathbf{N}_e$. The direction of the C line (cf. equation 3 for the vorticity defining the direction of a dislocation) is [25]

$$\mathbf{N}_{\mathrm{C}} = \tfrac{1}{2}\,\mathrm{Im}\,\nabla(\mathbf{E}^{*}\cdot\mathbf{E}^{*})\wedge\nabla(\mathbf{E}\cdot\mathbf{E}) = \nabla\left(P^2-Q^2\right)\wedge\nabla(\mathbf{P}\cdot\mathbf{Q}). \qquad (18)$$

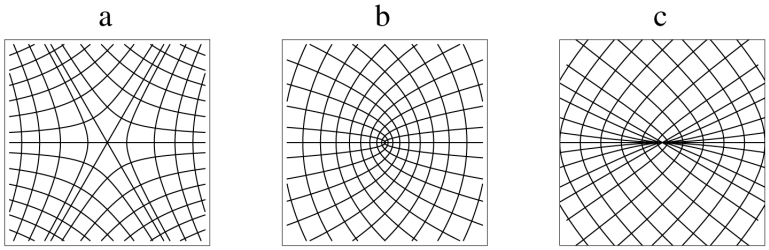

Figure 6. Patterns of axes of ellipses near a C singularity. (a) star (index -1/2); (b) lemon (index +1/2); (c) monstar (index +1/2).

The second type of polarization singularity occurs at places **r** where the ellipses degenerate to lines, that is, where the vectors **P** and **Q** are parallel. These are called L singularities, characterized by

$$\mathrm{Im}\,\mathbf{E}^{*}\wedge\mathbf{E}=2\mathbf{P}\wedge\mathbf{Q}=0\quad(\text{L singularity}). \tag{19}$$

For a line in space, the normal is undefined, and indeed $\mathbf{N}_e$ in (14) vanishes when (19) holds; in (14), the short-axis vector $\mathbf{E}_-$ vanishes, and the long axis $\mathbf{E}_+$ is parallel to **P** or **Q**. Parallelism of two three-dimensional vectors corresponds to two conditions, so for general complex vector fields in space the L singularities are *lines*. However, parallelism of two two-dimensional vectors corresponds to only one condition, so for general complex vector fields in two dimensions the L singularities are also *lines*, and for transversely polarized fields in space (e.g. paraxial optical fields) the L singularities are *surfaces*.

An L singularity is characterized by the pattern of (very thin) polarization ellipses close to it. In the general three-dimensional case, this can be described [24] in terms of the short axis $\mathbf{E}_-$ of the ellipses in a plane transverse to the L line and perpendicular to **P** or **Q**. The stable patterns are the Poincaré singularities (figure 7) near a zero of a vector field in the plane, with index +1 (lines that are elliptical or radial), or -1 (lines that are hyperbolic) (the patterns can be generated in the $\mathbf{R}=(x, y)$ plane from (14) by choosing $\mathbf{P}=(\mathbf{A}\cdot\mathbf{R},1)$, $\mathbf{Q}=(\mathbf{B}\cdot\mathbf{R},1)$ where **A** and **B** are 2x2 matrices).

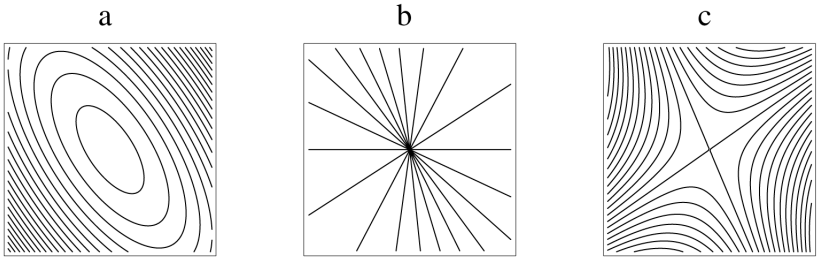

Figure 7. Pattern of short axis of ellipses near an L line in three dimensions. (a) and (b) have index +1, (c) has index -1.

In three dimensions, an L line need not be parallel to the ellipse axis $\mathbf{E}_+$ (i.e. parallel to **P** or **Q**). The direction of the L line is [25]

$$\mathbf{N}_{\mathrm{L}}=\nabla_{\mathrm{a}}\wedge\nabla_{\mathrm{b}}\left(\mathbf{N}_{\mathrm{e,a}}\wedge\mathbf{N}_{\mathrm{e,b}}\cdot\mathbf{e}_{\mathbf{P}}\right), \tag{20}$$

where $\mathbf{N}_e$ is given by (14), the suffixes a and b indicate the quantities on which the gradient operators act, and $\mathbf{e}_{\mathbf{P}}$ is the common direction of **P** and **Q**.

For both C and L singularities, alternative interpretations are possible, in terms of extreme values of an associated spin, or as matrix degeneracies [25].

The dislocations and polarizations of scalar and vector fields are related in several ways. We have already remarked that the C singularities of any vector field **E** can be regarded as dislocations in the associated scalar field $\psi=\mathbf{E}\cdot\mathbf{E}$. Similarly, any scalar field ψ possesses C and L singularities, generated by the associated vector field $\mathbf{E}=\nabla\psi$.

6. HANSEN AND THE TIDAL CURRENTS

Water is incompressible, so in the tides the vertical motion $z(\mathbf{r},t)$ (equation 11) must be accompanied by a horizontal flow; this is the tidal current. By continuity, the velocity $\mathbf{u}(\mathbf{r},t)$ of the tidal current (assumed uniform over the depth $D(\mathbf{r})$ of the ocean, for simplicity) is related to $z(\mathbf{r},t)$:

$$\partial_t z(\mathbf{r},t) = -\nabla\cdot\big[D(\mathbf{r})\mathbf{u}(\mathbf{r},t)\big]. \tag{21}$$

For harmonic motion, as in the M_2 tide, **u** can be generated by a complex vector field **E** according to (13), in the same way that z is related to the complex scalar ψ according to (11). Thus (21) can be written

$$\psi(\mathbf{r}) = \frac{\mathrm{i}}{\omega}\nabla\big[D(\mathbf{r})\mathbf{E}(\mathbf{r})\big]. \tag{22}$$

Evidently the tidal currents determine the height of the tide, but not conversely; therefore the tidal currents contain additional information, and it is interesting to study them.

The complex vector field $\mathbf{E}(\mathbf{r})$ of the tides determines the ellipse repeatedly described by the velocity of the tidal current at the point **r**. If **E** did not depend on **r**, and if there were no secular ocean currents, this velocity ellipse would drive each water particle in a similar ellipse, but with the long and short axes reversed. However, **E** does depend on **r**, and the variation would cause water particles to drift nonadiabatically according to the ellipses at different points, in ways that would be quite complicated, even chaotic - if it were not for the secular currents (e.g. the Gulf Stream), that in fact dominate the long-time motion of the water in the real oceans.

The pattern of velocity ellipses for the tidal currents of the North Sea was studied extensively by Hansen [31] (see also [30]). In a tour de force combining observations with Laplace's dynamical equations and (22), he was able to plot crosses representing the magnitudes and directions of the axes of the ellipses at points on a grid covering the sea. To get a clearer picture of the currents, he also plotted contours of a quantity, related to the eccentricity of the ellipses, equivalent to the local expectation value of photon spin in optics [25], namely $S_z=\mathbf{e}_z\cdot\mathbf{N}_e/\mathbf{E}^*\cdot\mathbf{E}$. Although he did not emphasise the polarizaton singularities, he did note the existence of points where $S_z=\pm1$ - in singularity terminology, these are the C points with left- and right-handed circular polarization - and the lines where $S_z=0$ - these are the L lines, where the polarization is linear. From this information, we can attempt to draw the orthogonal net of directions of $\mathbf{E}_\pm$ in the ellipse field (figure 8). In the region shown, there are three polarization singularities, two with index -1/2, that is stars, and one with index +1/2; I have drawn this as a lemon although the possibility of its being a monstar cannot be ruled out (on probabilistic grounds [26] we expect monstars to be rare).

Hansen went further, and realized (cf. the remarks at the end of section 5) that there is another field of ellipses, distinct from that associated with the tidal currents, associated with the complex slope vector $\nabla\psi$ of the tide wave. He called this the inclination field of the tide, and plotted its crosses and eccentricity contours.

7. ACKNOWLEDGEMENTS

These recent perspectives on phase and polarization singularities have been reached in close collaboration with Mark Dennis, for which I thank him; I also thank John Nye for helpful conversations. This paper was written during a generously supported visit to the physics department of the Technion, Haifa.

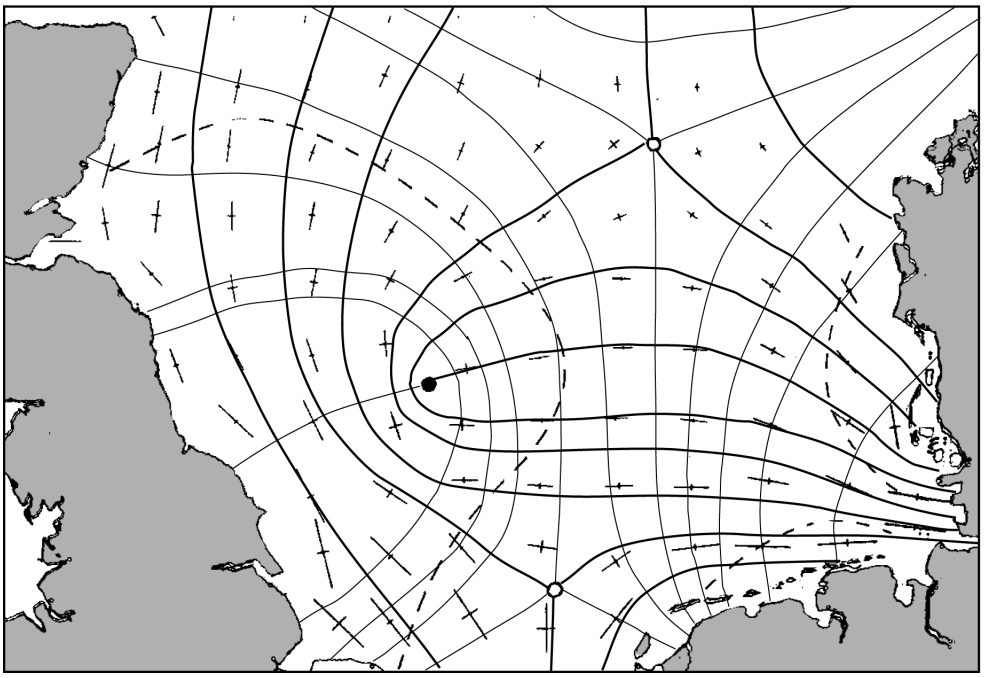

Figure 8. Orthogonal net of directions of the long axes (thick lines) and short axes (thin lines) of ellipse field (crosses) of the tidal currents in the North Sea (adapted from data of Hansen [31]). Circles (open and filled for the two senses of polarization) denote the C singularities (a lemon and two stars), and the dashed lines denote the L singularities.

8. REFERENCES

1. M. S. Soskin (ed), "Singular Optics," in *SPIE*, vol. 3487. Washington: Optical Society of America, 1998.
2. M. Vasnetsov and K. Staliunas, *Optical vortices*. Commack, New York: Nova Science Publications, 1999.
3. J. F. Nye, *Natural focusing and fine structure of light: Caustics and wave dislocations*. Bristol: Institute of Physics Publishing, 1999.
4. M. V. Berry and M. R. Dennis, "Phase singularities in isotropic random waves," *Proc. Roy. Soc. Lond. A456*, pp. 2059-2079, 2000.
5. A. Sommerfeld, *Optics: Lectures on Theoretical Physics, vol. 4*. New York: Academic Press, 1950.
6. D. E. Cartwright, *Tides: a scientific history*. Cambridge: University Press, 1999.
7. J. F. Nye and M. V. Berry, "Dislocations in wave trains," *Proc. Roy. Soc. Lond. A336*, pp. 165-90, 1974.
8. M. V. Berry, "Much ado about nothing: optical dislocation lines (phase singularities, zeros, vortices...)," in ref. 2.
9. I. Freund, "Optical vortex trajectories," *Optics Communs. 181*, pp. 19-33, 2000.
10. J. F. Nye, "The motion and structure of dislocations in wavefronts," *Proc. Roy. Soc. Lond. A378*, pp. 219-239, 1981.
11. I. Newton, *Opticks: or a Treatise of the Reflections, Inflections and Colours of Light*, 2nd ed. Mineola, N.Y.: Dover, 1952.
12. A. I. Khishniak, S. Anokhov, P., R. A. Lymarenko, M. S. Soskin, and M. V. Vasnetsov, "The structure of edge-dislocated wave originated in plane-wave diffraction by a half-plane," *J. Opt. Soc. Amer. A17*, In press, 2000.
13. W. Braunbek and G. Laukien, "Features of refraction by a semi-plane," *Optik. 9*, pp. 174-179, 1952.
14. E. Madelung, "Quantentheorie in hydrodynamische Form," *Z. für Phys. 40*, pp. 322-6, 1926.
15. P. Holland, *The Quantum Theory of Motion. An Account of the De Broglie-Bohm Causal Interpretation of Quantum Mechanics*. Cambridge: University Press, 1993.
16. W. Whewell, "Essay towards a first approximation to a map of cotidal lines," *Phil. Trans. Roy. Soc. Lond.*, pp. 147-236, 1833.
17. W. Whewell, "On the results of an extensive series of tide observations," *Phil. Trans. Roy. Soc. Lond.*, pp. 289-307, 1836.
18. A. Defant, *Physical Oceanography*, vol. 2. Oxford: Pergamon, 1961.
19. M. V. Berry, "Wave dislocations in nonparaxial Gaussian beams," *J. Modern Optics. 45*, pp. 1845-1858, 1998.

20. M. V. Berry and M. Robnik, "Quantum states without time-reversal symmetry: wavefront dislocations in a nonintegrable Aharonov-Bohm billiard," *J. Phys. A*, vol. 19, pp. 1365-1372, 1986.
21. R. J. Mondragon and M. V. Berry, "The quantum phase 2-form near degeneracies: two numerical studies," *Proc. Roy. Soc. Lond. A424*, pp. 263-278, 1989.
22. G. B. Airy, "Tides and Waves," in *Encyclopedia Metropolitana*, vol. 5. London, 1845, pp. 241-396.
23. E. W. Schwiderski, "Global ocean tides, part II: The semidiurnal principal lunar tide (M_2). Atlas of tidal charts and maps," Naval surface weapons center, Silver Spring, Maryland NSWC TR 79-414, 1979.
24. J. F. Nye and J. V. Hajnal, "The wave structure of monochromatic electromagnetic radiation," *Proc. Roy. Soc. Lond. A409*, pp. 21-36, 1987.
25. M. V. Berry and M. R. Dennis, "Polarization singularities in isotropic random waves," *Proc. Roy. Soc. Lond.A457*, pp. 141-155, 2001.
26. M. V. Berry and J. H. Hannay, "Umbilic points on Gaussian random surfaces," *J. Phys. A10*, pp. 1809-21, 1977.
27. I. R. Porteous, *Geometric differentiation: for the intelligence of curves and surfaces*. Cambridge: University Press, 1994.
28. M. Born and E. Wolf, *Principles of Optics*. London: Pergamon, 1959.
29. M. V. Berry, R. Bhandari, and S. Klein, "Black plastic sandwiches demonstrating biaxial optical anisotropy," *Eur. J. Phys. 20*, pp. 1-14, 1999.
30. J. F. Nye, J. V. Hajnal, and J. H. Hannay, "Phase saddles and dislocations in two-dimensional waves such as the tides," *Proc. Roy. Soc. Lond. A417*, pp. 7-20, 1988.
31. W. Hansen, *Gezeiten und Gezeitenströme der halbtägigen Hauptmondtide M_2 in der Nordsee*. Hamburg: Deutsche Hydrographisches Institut, 1952.